

# Quantum Phase Transitions in Anti-ferromagnetic Planar Cubic Lattices

Cameron Wellard<sup>1</sup> and Román Orús<sup>2</sup>

<sup>1</sup>*Centre for Quantum Computer Technology, School of Physics,  
University of Melbourne, Victoria 3010, Australia.*

<sup>2</sup>*Dept. d'Estructura i Constituents de la Matèria, Univ. Barcelona, 08028, Barcelona, Spain.*

(Dated: 30th October 2018)

Motivated by its relation to an  $\mathcal{NP}$ -hard problem, we analyze the ground state properties of anti-ferromagnetic Ising-spin networks embedded on planar cubic lattices, under the action of homogeneous transverse and longitudinal magnetic fields. This model exhibits a quantum phase transition at critical values of the magnetic field, which can be identified by the entanglement behavior, as well as by a Majorization analysis. The scaling of the entanglement in the critical region is in agreement with the area law, indicating that even simple systems can support large amounts of quantum correlations. We study the scaling behavior of low-lying energy gaps for a restricted set of geometries, and find that even in this simplified case, it is impossible to predict the asymptotic behavior, with the data allowing equally good fits to exponential and power law decays. We can therefore, draw no conclusion as to the algorithmic complexity of a quantum adiabatic ground-state search for the system.

PACS numbers: 03.67.-a, 03.65.Ud, 03.67.Lx, 03.67.Mn, 05.50.+q, 05.50.Fh

Quantum many bodied systems are of increasing interest in modern physics, particularly systems that exhibit a quantum phase transition (QPT). The nature of the quantum correlations between the components of these systems has been the subject of several recent studies [1, 2, 3, 4, 5, 6, 7, 8, 9, 10, 11, 12, 13, 14], with the suggestion that systems in the vicinity of the critical point are highly entangled. In this work we consider the phase-structure of a spin-model for which finding the ground state can, for certain parameters, be proven to belong to the complexity class  $\mathcal{NP}$ -hard [15]. We detect the presence of a QPT between paramagnetic and anti-ferromagnetic phases and find that this transition is accompanied by a peak in the entanglement between different parts of the system with a scaling behavior that makes it hard to simulate classically [8, 14, 16, 17]. Additionally, for the simplest realization of the spin network, we have calculated the minimum energy gap for networks of up to  $N = 24$  spins. The data accommodates equally good fits to both exponential and power law decays, allowing no conclusion to be formulated as to the efficiency of adiabatic quantum algorithms in solving this classically  $\mathcal{NP}$ -hard problem. Finally, we study the effects of frustration in these spin networks, which adds an extra element of complexity, altering the phase structure of the system.

The Hamiltonian under consideration is

$$H = \sum_{\langle i,j \rangle} \sigma_i^z \sigma_j^z + B \sum_{i=1}^N \sigma_i^z + \Gamma \sum_{i=1}^N \sigma_i^x, \quad (1)$$

where the sums over  $\langle i, j \rangle$  and  $i$  run over the edges, and vertices respectively, of the particular lattice under study. The parameters  $B$  and  $\Gamma$  are respectively the longitudinal and transverse magnetic fields, and  $N$  is the number of

spins (qubits), each associated with an individual vertex of the lattice. Spin networks of various planar cubic geometries are considered [15], and a QPT between paramagnetic (large fields), and anti-ferromagnetic (low fields) phases is expected in each case. The phase diagram of the system is shown schematically in Fig.1.

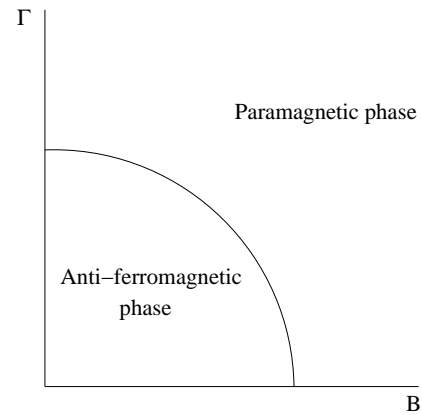


Figure 1: Expected phase diagram in the  $(B, \Gamma)$  plane for the systems under study.

A ground-state search for this system, over the entire set of planar cubic lattices, can be shown to be  $\mathcal{NP}$ -hard for the parameters  $B = 1, \Gamma = 0$ , due to a direct mapping to the problem of identifying the maximum cardinality of a stable set, for planar cubic graphs [15]. In the presence of extremely high fields however, the ground state is clearly trivial regardless of the size of the system, being simply given by the state in which all spins are aligned with the field. This gives rise to the possibility of performing the, classically  $\mathcal{NP}$ -hard, ground state search quantum mechanically, using a quantum adiabatic algorithm. The procedure would be as follows: set the

quantum register into the paramagnetic ground state of the system, with a very large magnetic field, and adiabatically change this field to the values  $B = 1, \Gamma = 0$ . Provided the evolution is adiabatic, the system is guaranteed to evolve to the ground state of this final Hamiltonian with a high probability. Clearly the evolution involves crossing the phase boundary, from the paramagnetic to the anti-ferromagnetic phase, and the time required to perform the procedure is determined by the energy spectrum at the critical point. It is, therefore, the scaling behavior of the energy spectrum at the critical point, that determines the computational cost of the quantum adiabatic ground-state search. This provides a strong motivation for studying the nature of the QPT in this system.

The set of all possible planar cubic graphs grows rapidly with the number of nodes on the graph, with the behavior of different instances varying considerably. We therefore find it convenient to begin the paper by focusing on a particular, simple, instance of the planar cubic graphs, which can be easily scaled. We then proceed to consider other particular instances, before finally considering the average behavior of the entire set. Our approach is numerical, and so we are restricted to small instances,  $N \leq 24$  for even the simplest cases, making it difficult to draw any conclusions about the asymptotic behavior of the system.

Possibly the simplest subset of the planar cubic lattices that can be easily scaled, are those consisting of two coupled rings, shown in Fig.2, which we refer to as the “ladder on a circle” geometry. As with cubic lattices in general, these lattices always contain an even number of nodes  $N$ , however, they can be divided into two classes. If there is an even number of nodes on each ring, the system contains no frustration, while if the rings contain an odd number of nodes, then the lattice is frustrated. Although this frustration does not scale with the size of the system, the number of frustrated edges in the ground state is two, regardless of the system size, and the two systems must have identical properties in the thermodynamic ( $N \rightarrow \infty$ ) limit, for the small system sizes considered here, the frustration does have some effect.

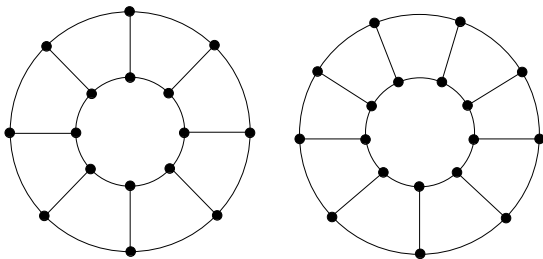


Figure 2: “Ladder on a circle” for  $N = 16$  (left) and  $N = 18$  (right). For  $N = 16$  the system is not frustrated, while for  $N = 18$  it exhibits frustration.

In the case of non-frustrated lattices the phase structure of the system is evident even from the small lattice sizes considered in this article,  $N \leq 24$ , with clear indicators of a QPT. Although the frustrated lattice must, in the thermodynamic limit, share the same phase diagram, the phase structure is more difficult to observe in small systems. This point is illustrated by considering the low-lying energy gaps of the system. Quantum phase transitions are marked by the vanishing of the first energy gap ( $\Delta_{12}$ ), the difference between the ground state and the first excited state energies. In the “ladder” geometry this gap is finite in the paramagnetic phase, decreasing abruptly to zero, in the thermodynamic limit, for the anti-ferromagnetic phase. In the non-frustrated system, the QPT is also marked by a clear minimum in the second energy gap  $\Delta_{13}$ , at the critical point, which can be easily observed for finite systems, as is shown in Fig.3 for  $N = 16$ . For the frustrated ladder however, the multiple degeneracy of the ground state in the anti-ferromagnetic phase implies that the minimum will only be manifest in some higher energy gap, exactly how high is dependent of the size of the system, making it far more difficult to observe.

Because of this compression of the energy levels at the critical points, it is the energy spectrum at this point that determines the minimum time-scale for adiabatic evolution between the two phases. In general the adiabatic time-scale is determined by the relation

$$\frac{|\langle e_n(t) | \partial H(t) / \partial t | e_1(t) \rangle|}{\Delta_{1n}^2} \ll 1, \quad (2)$$

where  $|e_n(t)\rangle$  is the  $n^{\text{th}}$  energy eigenstate of the Hamiltonian  $H(t)$ . In the case of the non-frustrated “ladder on a circle”, the lowest energy level for which the matrix element in the numerator does not vanish, is the third energy level. In any case, because the ground state in the anti-ferromagnetic phase is doubly degenerate, exciting the second energy eigenstate during adiabatic evolution from the paramagnetic phase does not compromise the evolution. It is therefore the second energy gap, the energy difference between the ground state and the third energy eigenstate, which determines the minimum time-scale for adiabatic evolution in this system. The scaling of this energy gap with the size of the lattice, then, determines the computational complexity of a quantum adiabatic ground state search for these lattices. In the case of the frustrated ladders however, the multiple degeneracy of the anti-ferromagnetic ground state implies that the relevant energy gap is higher, exactly how high depends on the size of the system, and so it is far more difficult to determine the required adiabatic evolution time for such a geometry.

We have analyzed the scaling behavior of the second energy gap for non-frustrated ladder geometries for system sizes up to  $N = 24$ . The data allow equally good

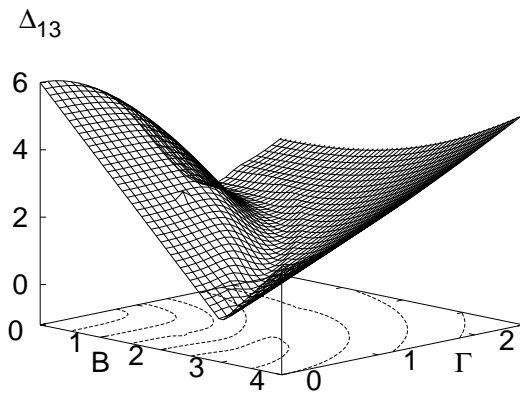


Figure 3: Phase diagram of the non-frustrated “ladder on a circle”, for  $N = 16$  spins. The energy gap between the ground and second excited state reveals the appearance of two well separated phases. The critical line numerically fits the law  $\Gamma = 1.93949 - 0.367302B + 0.237182B^2 - 0.106107B^3$ .

fits to either exponential or power law decays of the gap with lattice size, allowing us to draw no conclusion as to the asymptotic behavior of the scaling. A confident determination of the scaling law in this case would involve the analysis of much bigger systems, which are clearly outside of our computational capabilities by the direct diagonalization techniques employed in this study. As a consequence, no conclusion can be formulated as to the efficiency of possible adiabatic quantum algorithms for a ground-state search for even this restricted subset of planar cubic lattices. The problem of computing the quantum adiabatic complexity of the the classically  $\mathcal{NP}$ -hard ground state of generic anti-ferromagnetic planar cubic systems with  $B = 1$  and  $\Gamma = 0$  [15, 20] is even more difficult. In this case the difficulty of determining a general scaling law for the energy gap using only a restricted number of small lattices is compounded by the fact that it is not *a priori* evident which energy gap determines the minimum evolution time. Different instances of planar cubic graphs, of the same size, can have vastly different degrees of frustration, and so different ground state degeneracies. The energy gap that determines the minimum adiabatic evolution time will therefore, in general, depend on the particular lattice under consideration.

The two magnetic phases can also be distinguished by the entanglement characteristics of their ground states. In the paramagnetic phase, the ground state is not entangled, whereas in the magnetically ordered phase, the ground state is highly entangled. The critical point is, therefore, marked by some change in the entanglement behavior. Indeed it has been argued that one of the signatures of a QPT is entanglement on all length scales at the critical point [2, 3, 4, 5, 6, 7, 8, 9, 10, 11, 12, 13, 14], in rough analogy to classical correlation functions in a

thermodynamic phase transition.

In this discussion we use an entanglement measure defined as the entropy of the reduced density matrix, which gives an indication of the entanglement between different blocks of particles. For instance, the single particle reduced density matrix obtained by tracing out all but one particle, will have an entropy which gives a measure of the level of entanglement between that particle and the rest of the system. Similarly, if we trace out half of the particles, the entropy of the reduced density matrix gives a measure of the total entanglement between the block of particles remaining, and those that have been traced out.

The ground state entanglement between a single spin and the remaining system, calculated in this way for a non-frustrated ladder, rises monotonically as the strength of the field is decreased, moving from the paramagnetic to the ordered phase, due the  $\mathbb{Z}_2$  symmetry of the system in the  $\Gamma \rightarrow 0$ ,  $B \rightarrow 0$  limit (the ground state for the “ladder geometry” is close to a GHZ state of  $N$  qubits for low values of  $\Gamma$  and  $B$ ). This degeneracy leads to some numerical noise in the data. As any linear combination of degenerate eigenstates is also an eigenstate, this implies that some quantities, including entanglement measures, which differ between the different ground states, become ill defined at this point, and depend on which state is chosen. Additionally, although actually non-degenerate for finite  $\Gamma$ , in larger systems the first energy gap may be too small for the diagonalization algorithm to resolve, leading similar problems for small values of  $\Gamma$ . This noise may be seen in some of the plots presented in this article, but we point out that wherever it is observed, the limiting behavior of the system is clear.

In contrast to the single particle entropy, the QPT is indicated by a peak in the entropy of the reduced density matrix of  $N/2$  connected particles  $S(\rho_{N/2})$ . In the case of the ladder geometries we have traced out the particles on one of the two rings, and the entanglement calculated in this fashion is shown in Fig.4. The QPT is therefore identified by a collective measure of entanglement, involving quantum correlations between large blocks of qubits.

The scaling of this entropy peak at the critical point with the size of the system, seems to be in agreement with an area law which predicts that the entanglement between two blocks of spins should scale as the size of the boundary between the blocks, measured in terms of the number of qubits. Note that, despite the fact that our configuration is planar, the particular geometry and spin partition we have chosen forces the scaling behavior of the entropy to be strongly linear, due to the linear number of short-range interactions we “cut” with the bipartition between the inner and outer ring [4, 5, 8, 14, 18, 19]. This result indeed implies that the ground state of the system at the critical point is close to a Valence Bond state, as described in [13]. The scaling of this entropy peak for

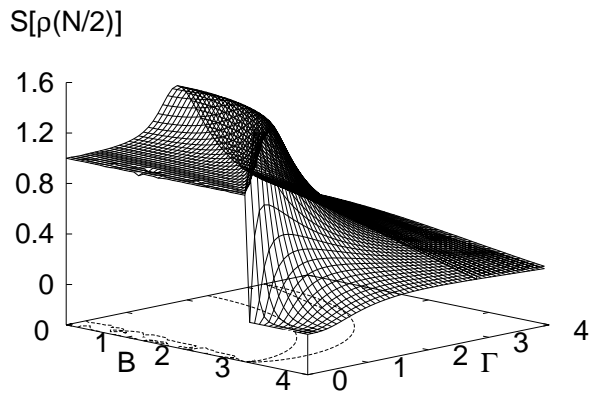


Figure 4: Entanglement entropy of the reduced density matrix for the particles on the inner (outer) ring, for  $N = 16$ . The peak indicates the crossing of the critical region in the  $(B, \Gamma)$  plane. The critical line numerically fits the law  $\Gamma = 1.93949 - 0.367302B + 0.237182B^2 - 0.106107B^3$ .

non-frustrated ladders, taken along the line  $B = 1$ , indicates that the scaling tends to obey  $S(\rho_{N/2}) \sim 0.08 N$  as the size of the system increases (see Fig.5). This behavior is similar to the linear law already found in [8] for the Exact Cover adiabatic quantum algorithm, and clearly differs from the logarithmic law found in [4, 5] for quantum spin chains. Entanglement scaling according to this particular bipartition of the system implies that even this simple planar model is able to produce an exponentially large amount of quantum correlations, as measured by the maximum rank of the reduced density matrices over all possible bipartitions. This number can be proven to be a measure of entanglement that controls the efficiency of certain protocols in order to classically simulate the system in a conventional computer. The results presented here imply that these classical simulation protocols would become inefficient due to the large amount of entanglement present in the system [8, 14, 16, 17].

Techniques from Majorization theory [21, 22, 23, 24, 25] have proven to be fruitful in characterizing the structure of the ground state across a QPT. We have chosen to calculate the  $2^N$  cumulants  $c_l = \sum_{i=1}^l p_i^\downarrow$  arising from the sorted probabilities  $p_i^\downarrow = |\langle i | \psi_g \rangle|^2$  - where  $|i\rangle$  is a quantum state, expressed in the  $z$ -basis (basis in which the Hamiltonian in Eq(1) is written),  $|\psi_g\rangle$  is the ground state of the system, and  $p_i^\downarrow$  are the probabilities sorted into decreasing order- at each step when varying the Hamiltonian parameters. The Majorization analysis of this set of probabilities has been useful in the study of efficiency in quantum algorithms [26, 27, 28]. Across the QPT on the line  $B = 1$ , we observe in Fig.6 that there exists a Majorization arrow in the direction of decreasing transverse magnetic field  $\Gamma$ . The phase transition is marked by a change in the cumulants at the critical point, reflecting

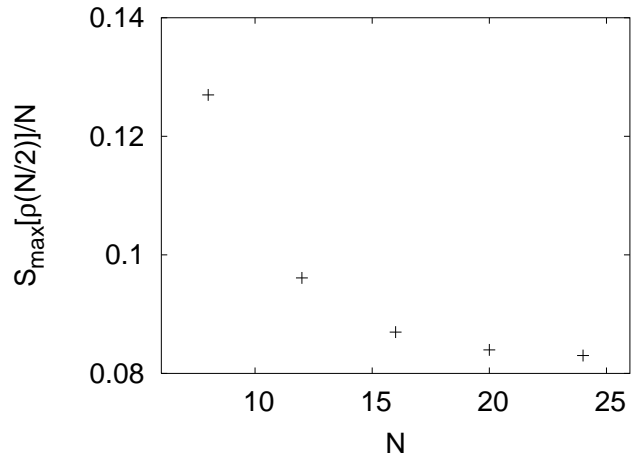


Figure 5: Maximum entanglement entropy per site between two rings of a non-frustrated ladder configuration as a function of the number of lattice sites, up to  $N = 24$ , along the line  $B = 1$ . For large  $N$  the quantity  $\frac{S_{\max}(\rho_{N/2})}{N}$  tends to a constant, which reveals an asymptotic linear scaling for the entropy peak.

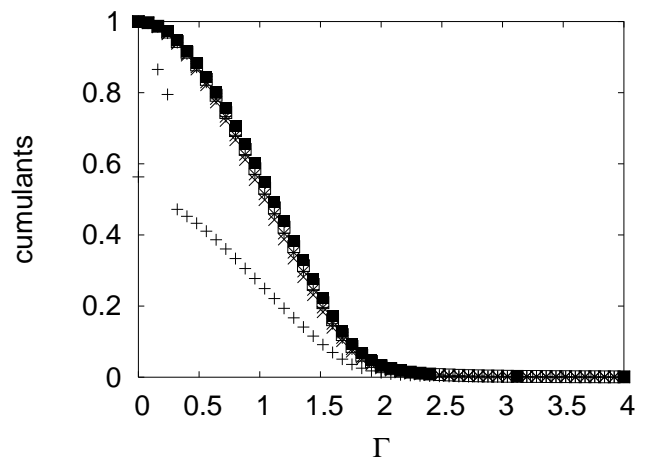


Figure 6: Majorization arrow for  $B = 1$  when decreasing  $\Gamma$ , for  $N = 16$ . There is a change in the behavior of the cumulants at the critical point  $\Gamma_c \sim 1.8$ . For simplicity only the first five cumulants are plotted.

the transition from a paramagnetic to a magnetically ordered phase. Step-by-step Majorization implies that the ground state is becoming increasingly ordered after each step in a very strong sense, at the precise level of each one of the probabilities, not just at the global level of expectation values such as the mean magnetization. An alternative Majorization analysis arises from the probability distribution obtained from the eigenvalues of the reduced density matrix of  $N/2$  particles,  $\rho_{N/2}$  [29]. In the case of the “ladder” geometry we have performed this analysis tracing out one of the two rings. The cumulants calculated according to this procedure also change their behavior at the critical point, this time decreasing as the

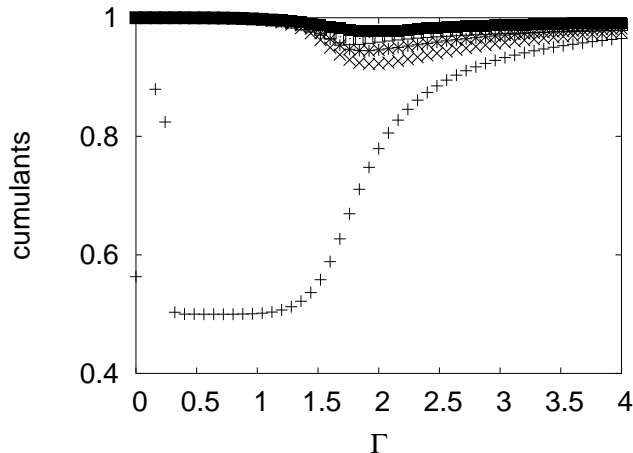


Figure 7: Majorization analysis of the eigenvalues of the density matrix  $\rho_{N/2}$  when tracing out one of the rings, when decreasing  $\Gamma$ , for  $N = 16$  and  $B = 1$ . There is a change in the behavior of the cumulants at the critical point  $\Gamma_c \sim 1.8$ . For simplicity only the first five cumulants are plotted.

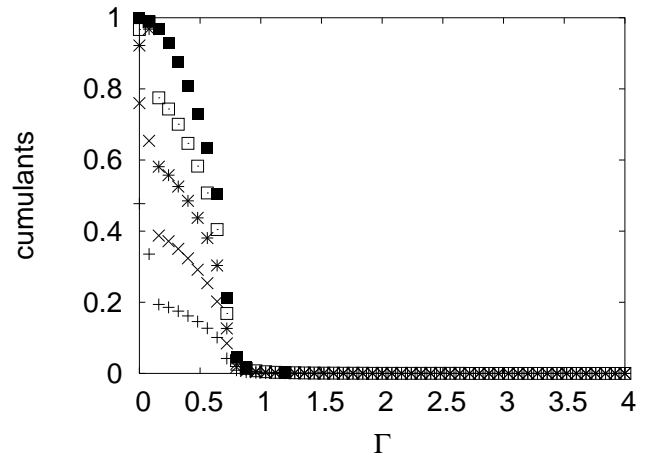


Figure 9: Majorization cumulants for the pentagonal lattice of  $N = 20$  spins, for  $B = 1$  when decreasing  $\Gamma$ . A change in their behavior is observed at the critical point  $\Gamma_c \sim 0.7$ . For simplicity only the first five cumulants are plotted.

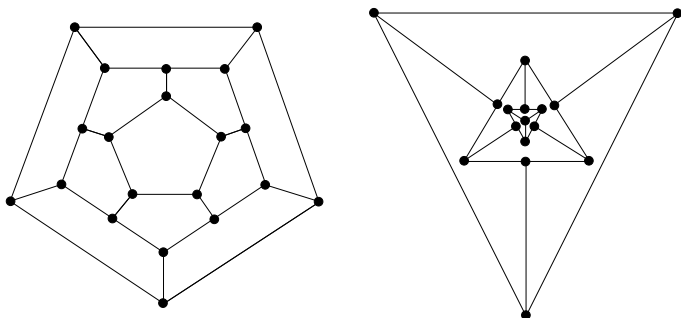


Figure 8: Pentagonal (left) and tetragonal (right) geometries for cubic planar lattices of  $N = 20$  and  $N = 16$  spins respectively.

field is decreased across the QPT. This can be observed in Fig.7.

Other planar cubic lattices of different geometries show similar behavior, with respect to these cumulants, in the critical region. For example, we have analyzed the two geometries shown in Fig.8 (which we call “pentagonal” and “tetragonal” geometries) for  $N = 20$  and  $N = 16$  qubits respectively. These geometries are easily scalable, and for small instances, highly frustrated, although the proportion of frustrated edges asymptotes to zero in the thermodynamic limit. These lattices also exhibit a QPT between paramagnetic and anti-ferromagnetic phases, corresponding to a compression of the high energy levels of the system at the points at which correlations, as measured by the entanglement entropy, are maximum [10].

The Majorization analysis for these lattices reveals similar results to the ones presented for the “ladder” geometry: for  $B = 1$  and when decreasing  $\Gamma$ , the cumulants

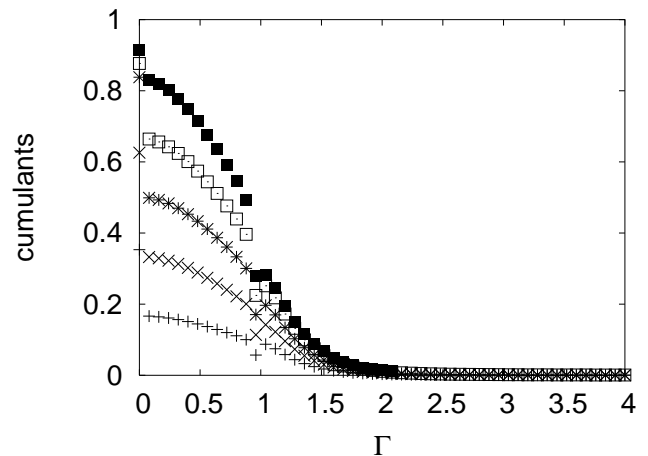


Figure 10: Majorization cumulants for the tetragonal lattice of  $N = 16$  spins, for  $B = 1$  when decreasing  $\Gamma$ . A change in their behavior is observed at the critical point  $\Gamma_c \sim 1.6$ . For simplicity only the first five cumulants are plotted.

obtained from the probabilities for the ground state, in the  $z$ -basis, increase at the critical point, as is observed in Fig.9 and Fig.10. In contrast to this, and in agreement with the results obtained for the ladder geometries, the Majorization behavior of the eigenvalues obtained from the reduced density operator  $\rho_{N/2}$ , decrease at the critical point, as is seen in Fig.11 and Fig.12.

To further illustrate our claims of Majorization signature for a QPT, we present results obtained using values calculated for all 1249 possible planar cubic graphs with  $N = 18$ , and averaged. In Fig.13 we show the lowest two energy gaps, the entropy of the reduced density matrix of a single particle (chosen at random), the entropy of the reduced density matrix of a block of  $N/2$

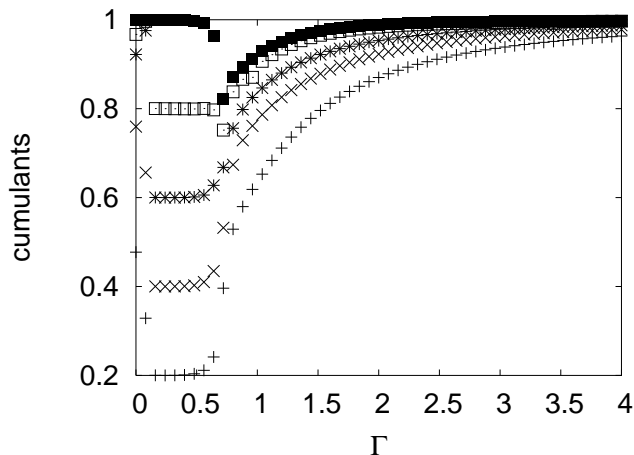


Figure 11: Majorization analysis of the eigenvalues of the density matrix  $\rho_{N/2}$  when tracing out half of the system, when decreasing  $\Gamma$ , for  $N = 20$  and  $B = 1$  on the pentagonal lattice. There is again a change in the behavior of the cumulants at the critical point  $\Gamma_c \sim 0.7$ . For simplicity only the first five cumulants are plotted.

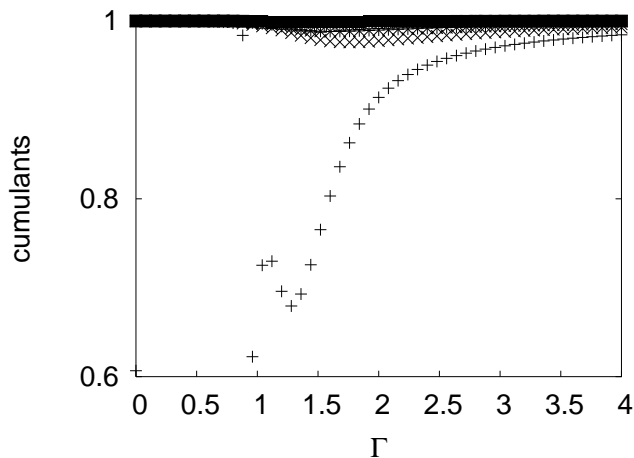


Figure 12: Majorization analysis of the eigenvalues of the density matrix  $\rho_{N/2}$  when tracing out half of the system, when decreasing  $\Gamma$ , for  $N = 16$  and  $B = 1$  on the tetragonal lattice. There is a change in the behavior of the cumulants at the critical point  $\Gamma_c \sim 1.6$ . For simplicity only the first five cumulants are plotted. Unavoidable numerical noise is present for the first cumulant close to  $\Gamma = 1$ .

connected spins (chosen at random), and the lowest cumulant as calculated using the Majorization procedures already discussed. The data were taken along the line  $B = 0.5$ , along which we expect a phase transition in all of the geometries. Our results show that all these quantities change abruptly at the same value of  $\Gamma$ , strongly suggesting the presence of a QPT.

To summarize, we have studied the quantum phase transition in anti-ferromagnetic planar cubic lattices un-

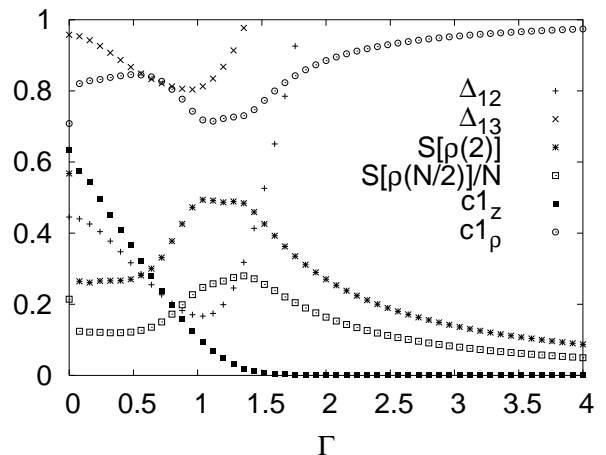


Figure 13: Here we plot various parameters calculated for all 1249 possible planar cubic lattices with  $N = 18$ , and averaged. The data were taken along the line  $B = 0.5$ , and each parameter exhibits a signature of a quantum phase transition. The parameters plotted include the first and second energy gaps  $\Delta_{12}, \Delta_{13}$ , each of which displays a clear minimum. The entropy of the reduced density matrix of a single spin (chosen at random)  $S[\rho(1)]$  and a block of  $N/2$  connected spins (again chosen at random) divided by  $N$   $S[\rho(N/2)]/N$ . Each of these quantities shows a peak at the critical region, between  $\Gamma = 1$  and  $\Gamma = 1.4$ . Finally we have plotted the lowest cumulants of a Majorization analysis based on the ordering of the ground state in the  $z$  basis,  $c1_z$ , and based on an ordering of the eigenvalues of the  $N/2$  particle reduced density matrix  $c1_\rho$ . The first of these shows a sudden increase, while the second exhibits a minimum on the vicinity of the QPT.

der the action of homogeneous magnetic fields. We have shown that techniques from quantum information science [30], such as the behavior of entanglement entropy or Majorization theory, can be directly applied to the study of quantum many-body systems, leading to new points of view in the study of quantum critical phenomena. Lattices of different geometries display phase diagrams with characteristic and differentiated anti-ferromagnetic and paramagnetic regions. Scaling laws for entanglement at the critical point seem to be in agreement with the area law, in a way that even the simplest planar models are able to provide exponentially large quantum correlations, as measured by the maximum rank of the reduced density matrices over all possible bipartitions. The understanding of the behavior of these systems is well characterized by the use of Majorization theory and the analysis of entanglement entropy, both of which reveal details about the transitions present in the models which are sometimes hard to be obtained by the study of the energy spectrum.

**Acknowledgments:** R.O. acknowledges financial support from projects MCYT FPA2001-3598, GC2001SGR-00065 and IST-1999-11053. The authors are grateful to the Les Houches School of Theoretical

Physics, where this work was initiated, and to discussions with L.C.L. Hollenberg, T.D. Kieu, N. Lambert, J. I. Latorre, A. Prats and E. Rico. Particular thanks to Wayne Haig (High Performance Computing System Support Group, Department Of Defence, Australia) for computational support.

- 
- [1] S. Sachdev, *Quantum phase transitions*, Cambridge University Press, Cambridge (1999).
- [2] T. J. Osborne, M. A. Nielsen, quant-ph/0202162.
- [3] A. Osterloh, L. Amico, G. Falci and R. Fazio, *Nature* **416**, 608 (2002), quant-ph/0202029.
- [4] G. Vidal, J. I. Latorre, E. Rico, A. Kitaev, *Phys. Rev. Lett.* **90**, 227902 (2003), quant-ph/0211074.
- [5] J. I. Latorre, E. Rico, G. Vidal, *Quant. Inf. and Comp.* **4**, 1 (2004) pp.048-092, quant-ph/0304098.
- [6] F. Verstraete, M. Popp, J. I. Cirac, *Phys. Rev. Lett.* **92**, 027901 (2004), quant-ph/0307009.
- [7] N. Lambert, C. Emary, T. Brandes, *Phys. Rev. Lett.* **92**, 073602 (2004), quant-ph/0309027.
- [8] J. I. Latorre, R. Orús, *Phys. Rev. A* **69**, 062302 (2004), quant-ph/0308042.
- [9] V. Murg, J. I. Cirac, *Phys. Rev. A* **69**, 042320 (2004), quant-ph/0309026.
- [10] H. L. Haselgrove, M. A. Nielsen, T. J. Osborne, *Phys. Rev. A* **69**, 032303 (2004), quant-ph/0308083.
- [11] J. Vidal, R. Mosseri, J. Dukelsky, *Phys. Rev. A* **69**, 054101 (2004), cond-mat/0312130.
- [12] Olav F. Syljassen, quant-ph/0312101.
- [13] F. Verstraete, M. A. Martín-Delgado, J. I. Cirac, *Phys. Rev. Lett.* **92**, 087201 (2004), quant-ph/0311087.
- [14] R. Orús, J.I. Latorre, *Physical Review A* **69**, 052308 (2004), quant-ph/0311017.
- [15] F. Barahona, *J. Phys. A: Math. Gen.* **15**, 3241-3253 (1982).
- [16] G. Vidal, *Phys. Rev. Lett.* **91**, 147902 (2003), quant-ph/0301063.
- [17] G. Vidal, *Phys. Rev. Lett.* **93**, 040502 (2004), quant-ph/0310089.
- [18] M. Srednicki, *Phys. Rev. Lett.* **71** (1993) 666-669, hep-ph/9303048.
- [19] D. Kabat and M. J. Strassler, *Phys. Lett. B* **329**, 46 (1994), hep-th/9401125; D. Kabat, *Nucl. Phys. B* **453**, 281 (1995), hep-th/9503016.
- [20] E. Farhi, J. Goldstone, S. Gutmann, M. Sipser, quant-ph/0001106.
- [21] R. F. Muirhead, *Proc. Edinburgh Math. Soc.* **21**, 144, (1903).
- [22] G. H. Hardy, J. E. Littlewood, G. Pólya, *Inequalities*, Cambridge University Press, 1978.
- [23] A. W. Marshall, I. Olkin, *Inequalities: Theory of Majorization and its Applications*. Acad. Press Inc., 1979.
- [24] R. Bhatia, *Matrix Analysis* Graduate Texts in Mathematics vol. 169, Springer-Verlag, 1996.
- [25] M. A. Nielsen, G. Vidal, *Quantum Information and Computation*, **1**, 76, (2001)
- [26] J. I. Latorre, M. A. Martín-Delgado, *Phys. Rev. A* **66**, 022305 (2002), quant-ph/0111146.
- [27] R. Orús, J. I. Latorre, M. A. Martín-Delgado, *Quantum Information Processing*, **4**, 283-302 (2003), quant-ph/0206134.
- [28] R. Orús, J. I. Latorre, M. A. Martín-Delgado, *European Physical Journal D* **29**, 119-132 (2004), quant-ph/0212094.
- [29] J.I. Latorre, C.A. Lutken, E. Rico, G. Vidal, quant-ph/0404120.
- [30] M. A. Nielsen, I. Chuang, *Quantum Computation and Quantum Information*, Cambridge University Press, 2000.